

PAPER • OPEN ACCESS

Numerical investigation of fluid flow and heat transfer in an electrical machine cooling system using nanofluids

To cite this article: S. Jayakumar and M. Sreekanth 2020 *IOP Conf. Ser.: Earth Environ. Sci.* **573** 012015

View the [article online](#) for updates and enhancements.



ECS **240th ECS Meeting**
Oct 10-14, 2021, Orlando, Florida

**Register early and save
up to 20% on registration costs**

Early registration deadline Sep 13

REGISTER NOW

Numerical investigation of fluid flow and heat transfer in an electrical machine cooling system using nanofluids

S.Jayakumar*, M. Sreekanth*

School of Mechanical Engineering, Vellore Institute of Technology Chennai

Email : manavalla.sreekanth@vit.ac.in

Abstract. The numerical simulation of an electric machine (E-machine) used for hybrid electric vehicle, electric vehicle, and plug-in electric vehicle is carried out to explore the impact of distinct kinds of coolants such as water and distinct nanofluids on the bracket housing cooling performance. Nanofluids are stable nanofiber and fluid particle suspensions. Recent research shows that these nanofluids have enhanced thermal conductivity and convection coefficients, are superior to pure fluid. The aim is to understand the heat transfer enhancement brought by different nanofluids. The present study suggests that the use of Ga-In-Sn (Gallium, Indium, and tin) as the coolant leads to higher efficiency of heat transfer compared to other nanofluids agents and base fluid. Results indicate increased heat transfer in the cooling of the electrical machine as shown by a significant reduction of ~ 30% in the operating temperature when using nanofluids compared to pure fluid implementation. With superior thermal characteristics and countless advantages, nanofluids are promising to meet the cooling requirements of the machine by a reduction in thermal resistance and maximum temperature.

Key words: Electrical machine · Nanofluids · Numerical Simulation · Heat Transfer Enhancement

1. Introduction

The thermal expansion or contraction on the E-machines are created by the dissipated losses of the system, which will heat individual machine parts such as end windings, rotor assembly, rotor magnets, and need to be cooled. The E-machines thermally protected by reducing local losses, i.e. induced eddy-current losses in the electrical conduction fields, iron cores, magnets, maintaining sleeves and/or using an efficient cooling system. Depending on the implementation, it is possible to use cooling systems with natural convection (completely enclosed non-ventilated), forced convection (air or fluid cooling) [1] or radiation cooling (for E-machine working in a vacuum). An E-machine's conjugate heat transfer analysis is generally considered a more complicated one in terms of the construction and precision of a device.

Heat is extracted through conduction, convection (natural and forced) and radiation. Thermal management of electrical devices is a three-dimensional issue that needs complicated heat extraction phenomena to be resolved; e.g. heat transfer through composite parts such as wound slot, the temperature drop across component interfaces and flow within end caps [2]. This research provides alternatives for effective heat extraction and thermal management of the electrical machines used in electric hybrid vehicles, electric vehicles and electric vehicle plug-in.

Numerous experiments were carried out on motor cooling using different methods of cooling. Matsuzaki et al [3], for example, used liquid nitrogen to improve motor cooling. For electric motors Davin et al. [4] used lubricating oil as a coolant. They investigated patterns of oil injection to increase the cooling capacity. Lim and Kim [5] have suggested an in-wheel motor oil spray cooling system in electric vehicles using a hollow shaft. King et al. [6] used water direction to cool the permanent synchronous high-speed magnet (PMSM) motor. For brushless DC motors, Kim et al. [7] used air-cooling by increasing cooling capacity with optimized coolant route optimization. Huang et al. [8] used oil-cooling system to lower traction machine operating temperature. Mudawar et al., meanwhile,



used spray cooling for a feasible thermal control approach for electronic hybrid vehicles [9]. Karim and Yus[10] developed effective method for water cooling electric motors. Zhang et al. [11] developed a 3D finite element model with ANSYS for the controlled temperature field of an air-cooled and water-cooled motor.

Based on the literature survey, it is observed that various methods of heat removal have been adopted in the thermal management of E-machines. However, none has considered different nanofluids as a coolant in the thermal management system of E-machines yet. Therefore, this paper aims to study the heat transfer aspects using nanofluids as a coolant flowing in the channel for the electric vehicle motor cooling module to improve the effective heat transfer areas between liquid-coolant and the bracket surface.

2. Boundary Conditions & Simulation Method

The velocity is zero at all limits for hydraulic boundary condition except the inlet and outlet of the channel. At the inlet, a uniform velocity is applied. The velocity is obtained from the Reynolds number. The Reynolds number ranges from 90 to 4500 for all coolants including water. Based on the Reynolds number the flow is laminar& turbulent. In calculation of the Reynolds number, the channel inlet diameter and coolant properties are used as follows

$$u = \frac{Re \cdot \mu}{\rho \cdot d_h} \quad (1)$$

Where d_{th} = hydraulic diameter. The flow is fully developed at the channel inlet as shown in the equation (2).

$$\frac{du}{dx} = 0, \quad \frac{dv}{dy} = 0, \quad \frac{dw}{dz} = 0 \quad (2)$$

For thermal condition, constant heat supply is assumed at the stator coil stack.

$$q = k \frac{dT}{dz} \quad (3)$$

Adiabatic boundary conditions apply to the entire solid region's bracket except the coupled wall. In the cooling passage, the flow is also presumed to be thermally fully developed as the change in temperature gradient along the channel's flow path is generally small. Therefore, the thermal boundary condition will not introduce large numerical error.

$$\frac{d^2T}{dx^2} = 0 \quad (4)$$

CFD simulation method is given in figure 1.

To solve fluid problem physics using CFD the problem physics can be represented by NavierStokes equation, it should be converted into discrete form. Simulation equations are solved through computers. These simulation results are compared and analysed with real problem.

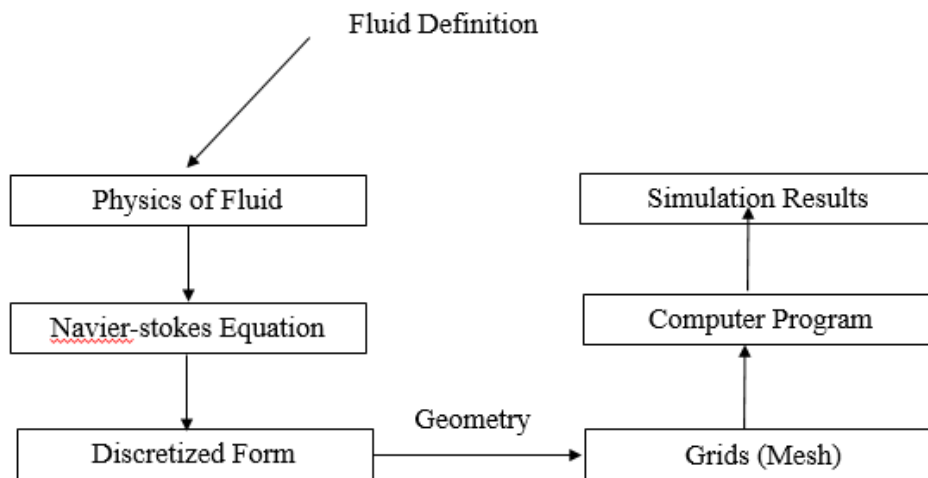


Figure 1. Schematic flow chart

3. CONVENTIONAL COOLANTS

Water is the most widely used coolant because when compared to other nanofluids it has a higher specific heat, thermal conductivity and reduced viscosity. However, due to its high freezing point and distribution after freezing, water is not used in closed loop systems. The frequently used standard cooling agents primarily categorized into two groups: (I) dielectric and (II) non-dielectric [12] liquids.

3.1 Dielectric coolants

This group of coolants contains several kinds of liquids, which are fluids based on aromatics, aliphatics, silicones, and fluorocarbons. Alkylated aromatics most frequently used as coolants because of cheaper and better results. Some aromatic coolants include benzene, diethyl benzene (DEB), toluene, and xylene.

Paraffinic and iso-paraffinic-type aliphatic hydrocarbons (including mineral oils) used in a variety of direct electronics cooling. In some application for cooling electronics, aliphatic poly alpha olefins (PAO)-based liquids are also used. Another common form of coolant known as silicone oils (e.g. Syltherm XLT) are liquids based on silicones. The primary benefit of this coolant class is its characteristics such as viscosity and freezing point governed by altering the length of the chain.

Fluorocarbon-based fluid that is widely known in the industry such as FC-77, FC-40, FC-72, and FC-87. These are non-flammable, inert, stable, non-reactive liquids. For cooling applications, FC-72 and FC-77 are most frequently used.

3.2 Non-dielectric coolants

Non-dielectric liquid coolants used frequently for cooling because of their superior properties compared to their dielectric variants. They are usually watery arrangements and thus present enhanced thermal conductivity and heat capacity, as well as relatively low viscosity. *Ethylene glycol (EG)*, *Water (W)*, and *these two mixtures (EG / W)* are commonly utilized as coolants for numerous gadgets. Other common non-dielectric coolants incorporate *NaCl solution*, *W / ethanol propylene glycol (PG)*, *water / methanol*, *potassium formate (KFO) solution*, and *liquid metals (e.g., Ga-In-Sn)* Table 1. The coolants characteristics and properties data can also found in the literature [13-16].

The nanofluids concentration is in the range of 10^9 to 10^{15} .

Table 1: Properties of various common liquids coolant [12] [13]

Coolants	Thermal conductivity (Wm-1K-1)	Specific heat (KJkg-1k-1)	Viscosity (mPas)	Density (kgm-3)
Water(W)	0.613	4.18	0.89	1000
Ethylene glycol(EG)	0.26	2.84	19.83	1109
W/EG (50/50/v/v)	0.36	3.285	3.8	1087
W/PG (50/50/v/v)	0.36	3.4	6.4	1062
W/methanol(60/40/w/w)	0.4	3.56	2	935
Aromatic(DEB)	0.14	1.7	1	860
Aliphatic(PAO)	0.137	2.15	9	770
Silicone(Syltherm XLT)	0.11	1.6	1.4	850
Fluorocarbon(FC-72)	0.054	1.09	0.65	1680
Fluorocarbon(FC-77)	0.06	1.17	1.13	1800
W/KFO(60/40/w/w)	0.53	3.2	2.2	1250
Dynalene HC-30	0.52	3.1	2.5	1275
Dynalene HC-50	0.505	2.7	3.2	1340
Ga-In-Sn	39	0.365	2.2	6363

4. Mesh Independent Study

The E-Machine was analysed for a flow rate of 3l / min to determine the accuracy of the CFD solution and to keep the computational costs low. The grid convergence study carried out by developing four different meshes with two fluids water, Ethylene glycol: with the E-Machine's coarse, medium, fine and very fine grid to predict the maximum stator temperature on standardized mesh cells to determine how the mesh quality affects CFD simulations results. As shown in Table 2, M1 contributes to a sensible forecast of the stator temperature, whereas M3, M4 is slightly higher than M2, M1. M4 is better to consider the effect of all nanofluids and used for numerical analysis. Since 5 million cells is fine for water, to be safe, all other fluids evaluated at 7 million cells.

Table 2. Grid size, Computation time and temperature

Grid resolution		Coarse M1	Medium M2	Fine M3	Very Fine M4
Cell Count(Million)		1	3	5	7
CFD Simulation time	Water(W)	32 min	1 hrs 20 min	2 hr 30 min	3 hr 20 min
	Ethylene glycol(EG)	28 min	1 hr 10 min	2 hr 25 min	3 hr 10 min
Maximum	Water(W)	59.955	59.206	59.271	58.965

Stator temperature (°C)	Ethylene glycol(EG)	97.406	96.810	96.320	96.102
-------------------------	---------------------	--------	--------	--------	--------

5. Numerical Method Validation

The reported research available in literature for the E-machine bracket cooling is very limited. In order to validate the numerical model for the fluid flow and heat transfer, a very similar experimental work carried out by Lee [17] is selected. The experimental layout consists of the nozzle and jet flow metering system, the heated impingement plate, and the digital image processing system. The wall temperature from stagnation region were measured at dimensionless nozzle to plate spacing of $L/D=2$. For the CFD simulations, an impingement surface heated uniformly with a constant heat flux and the jet-to-nozzle as shown in figure 2 considered.

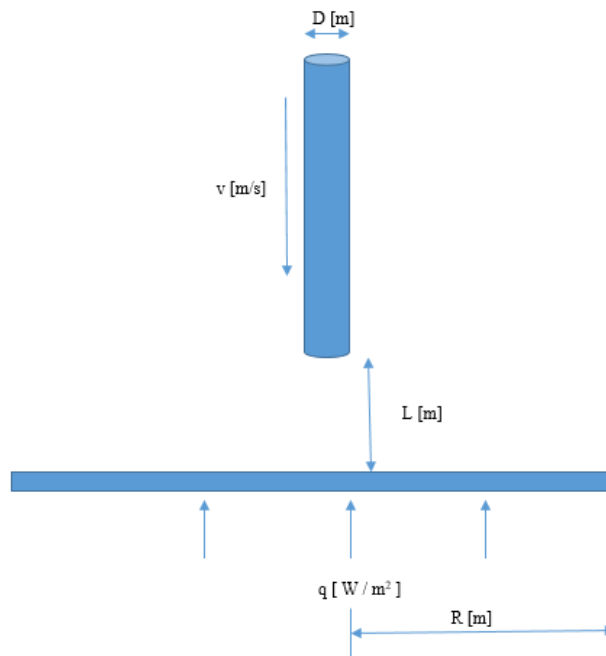


Figure 2. Geometry of impingement surface

The numerical models selected for the fluid flow and heat transfer investigated using Ansys Fluent to validate results obtained from the software. Results obtained show good agreement with the published paper by Lee [17]. A superposed plot, figure 3, of wall temperature along the heated surface shows a maximum difference of 11% between the published work and the present work for $Re = 20000$ and heat flux $q=100 \text{ W m}^{-2}$. The values of wall temperature show good agreement with experimental data from the stagnation points along the distance R . The maximum deviations in the wall temperature observed from $R/D = 3.5-4$. Therefore, the numerical model adopted for the E-machine CFD simulations is satisfactory.

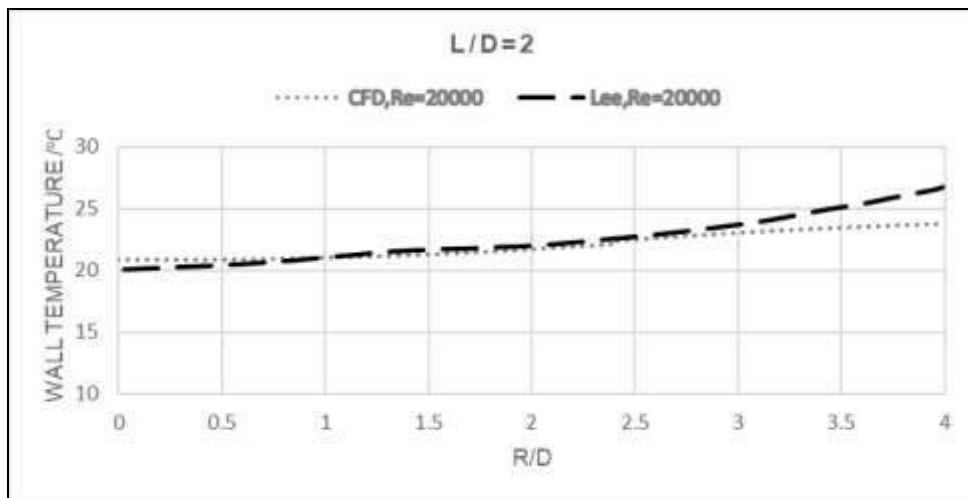


Figure 3. Variation of the wall temperature for L/D=2

6. Thermal Analysis

E-Machine's thermal model is solved with commercial Ansys Fluent software. The computational domain modelling is performed by Ansys meshing, the design of fluid passage and brackets in 3-D design. Model detail involves the specification of nanofluids (thermal conductivity k , specific heat c_p , viscosity μ , density ρ , etc.) as shown in Table 1. As operating parameters corresponding to the real world-working situation at idle rpm, a flow rate of 3L / min, stator loss (corresponding to quarter model) selected as in Table 3.

Table 3: Simulation Input Data

<i>Inlet mass flow (L/min)</i>	<i>3</i>
<i>Inlet temperature (K)</i>	<i>298.15</i>
<i>Convergence criteria</i>	<i>10^{-4}</i>
<i>Wall function</i>	<i>Enhanced Treatment</i>

A forced liquid cooling system motor generator is implemented and analysed. Figure 4, 5 shows the E-Machine's 3D quarter model. The model comprises of a simplified stator stack, front bracket, rear bracket and passage of fluids.

Some assumptions are made as follows to simplify the numerical calculation:

1. Both liquid flow and thermal transfer are in a steady state.
2. The fluid is incompressible in a single phase.
3. All surfaces of the brackets exposed to the surrounding area are insulated except the bracket and stator contact wall where constant heat source boundary conditions simulate heat generation.
4. Uniform flow of heat from the wall.
5. Uniform inlet velocity.
6. Due to forced convection and reduced working temperature, negligible radiation thermal transfer.
7. Flow is fully developed and the inlet, outlet regions are extended for 5, 7 times inlet hydraulic diameter d_h . [18]
8. Fluid properties are not depending on temperature [19].

The unstructured mesh used shown in Figure 6 and it includes about 7 million cells of the tetrahedral layer with prism. A dual adaptation refinement algorithm, Realizable $k-\epsilon$ model has been implemented to solve the thermal and flow problem.

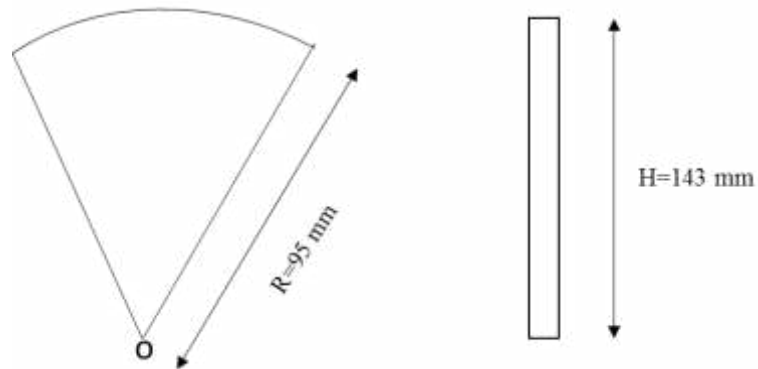


Figure 4. Geometry of E-machine

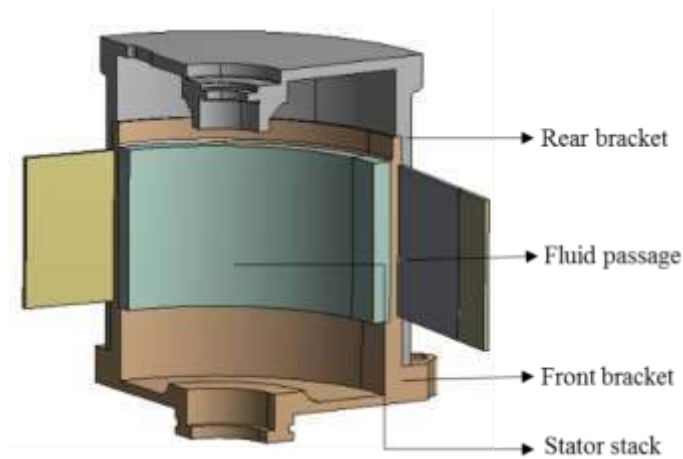


Figure 5. 3D Quarter model of E-Machine

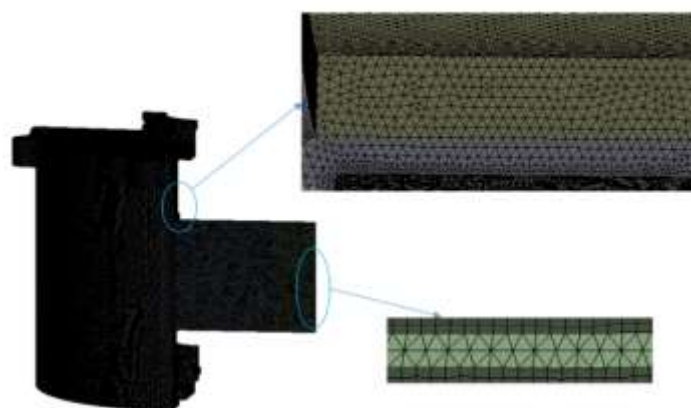


Figure 6. Mesh model of E-Machine

7. Results and Discussion

The findings are provided with heat conduction and forced convection being taken into consideration. The numerical solutions evaluated by the mathematical model integration show the heat transfer behaviour around the brackets. Figures 7 to 13 show the graphs & temperature field of the front, rear bracket & stator stack respectively i.e. the fluids within the fluid passage and the temperature field.

The fluid accumulates heat from the bracket's hot surface during the flow. At the outlet, some nanofluids have a temperature close to the inlet temperature, especially at the middle. This can be explained by the fact that the fluids in the centre of the channel have a greater velocity than the liquids near the brackets. In other words, as a focused jet, the fluids that flow through the cooling passage. As the flow pass between the brackets, it loses its efficiency and as time advances, the housing becomes progressively hotter.

7.1 Temperature and thermal resistance of nanofluids

Other surfaces are treated as a wall; the working fluid that entered the channel was heated because of the continuous heat source applied to the stator stack. From figure 7,8 & 9 it can be noticed that the Aliphatic nanofluid has the highest average temperature at the front bracket, rear bracket wall, stack which is around 93°C, 85°C & 113°C. Ga-In-Sn had been used in comparison with other nanofluids and it can be seen that when Ga-In-Sn was used, the surface temperature was lower than when other nanofluids were used as the working fluid. When using Ga-In-Sn as the working fluid, it indicates a temperature decrease of approximately ~30% of temperature reduction compared to pure water. Also from the contour, the temperature distribution along the surface of the bracket is uniform it means by using Ga-In-Sn the cooling is uniform the thermal runaway limited. However, in case of other nanofluids the temperature gradient along the surface is high. From figure 7 the average temperature of nanofluids such as Ga-In-Sn, Dynalene HC-30 and Dynalene HC-50 are in the range of 20-40 °C for the front bracket. For the remaining nanofluids the average temperature of front bracket is in the range of 40-100 °C.

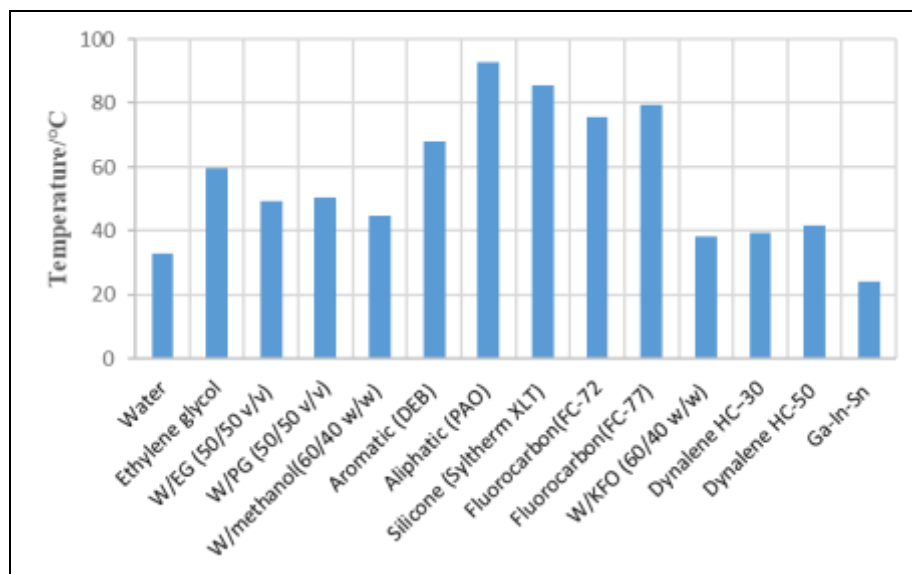


Figure 7. Influence of nanofluids on average temperature of front bracket

From figure 8 the average temperature of nanofluids such as W/KFO (60/40 w/w), W/methanol (60/40 w/w), W/EG (50/50 v/v), W/PG (50/50 v/v), Dynalene HC-30 and Dynalene HC-50 are in the range of 30-45 °C for the rear bracket. For the remaining nanofluids the average temperature of rear bracket is in the range of 45-90 °C. From figure 9, the stator stack temperature is below 40 °C for Ga-In-Sn.

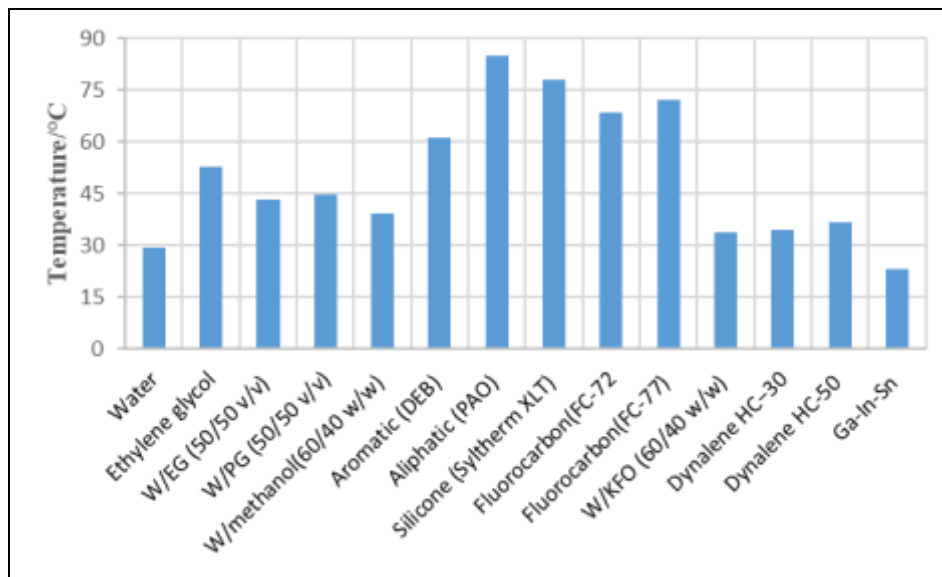


Figure 8. Influence of nanofluids on average temperature of rear bracket

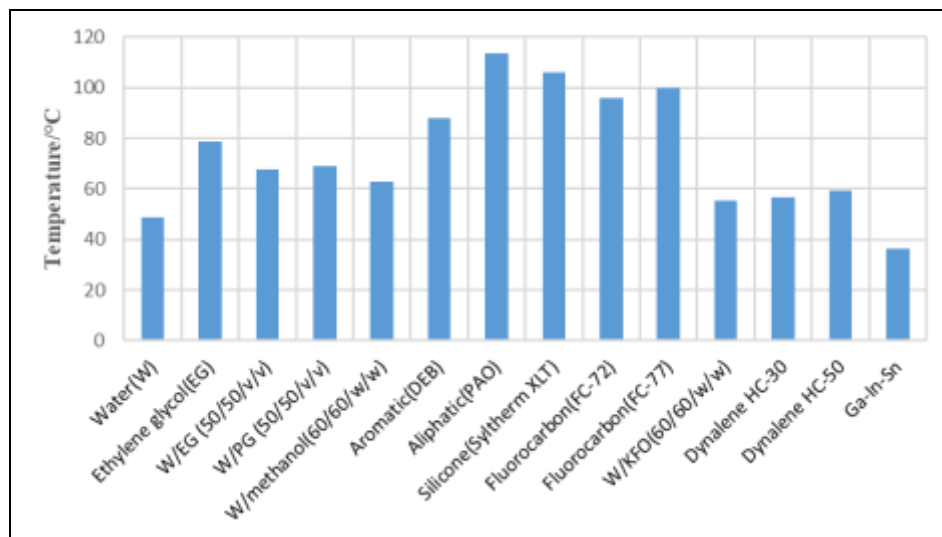


Figure 9. Influence of nanofluids on average temperature of stator stack

From figure 10, the thermal resistance of $0.24^{\circ}\text{C}\text{W}^{-1}$ observed for aliphatic nanofluid, the heat transfer from brackets to fluid is minimal when compared with other nanofluids. The Ga-In-Sn found to have good heat transfer enhancement with minimal thermal resistance of $0.028^{\circ}\text{C}\text{W}^{-1}$. For the remaining nanofluids from water to dymalene the thermal resistance falls in the range $0.050\text{-}0.24^{\circ}\text{C}\text{W}^{-1}$.

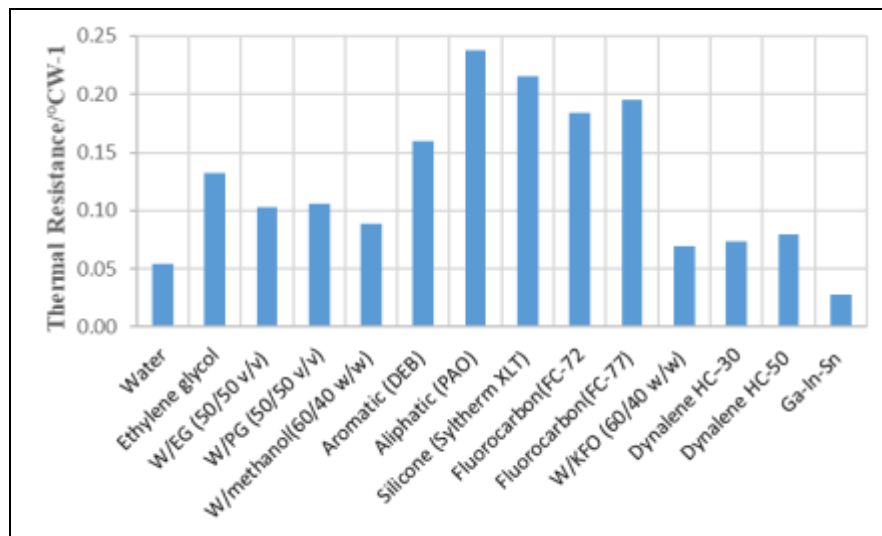


Figure 10. Influence of nanofluids on thermal resistance

Figure 11, 12 & 13 also demonstrate the growth of the surface temperature profile for different nanofluids in the same typical setup between the two brackets. The profiles shown demonstrates the fluid's gradual temperature rise as the fluid flows towards the channel's periphery. It is evident that there is no uniform temperature distribution in the brackets.

Overall, significant rises in overall heat transfer rates of 589.6W was found with the use of Ga-In-Sn nanoparticles. In all cases, the front bracket observed to have higher temperature when compared with rear bracket. For the remaining coolant nanofluids, the temperature of the housing bracket falls in the range of 23-85 °C.

In the first case (a) the temperature distribution along the surface is non-uniform on both the front and rear bracket. High temperature gradient of 30 °C observed near the inlet region of the stator stack, after the inlet region uniform temperature distribution is observed. Similar thermal behaviour observed for all nanofluids from (b)-(o) with thermal gradient from 10- 40 °C for the both the front & rear brackets. Only for Ga-In-Sn the temperature distributions is uniform and have reduced thermal runaway when compared with other nanofluids and water.

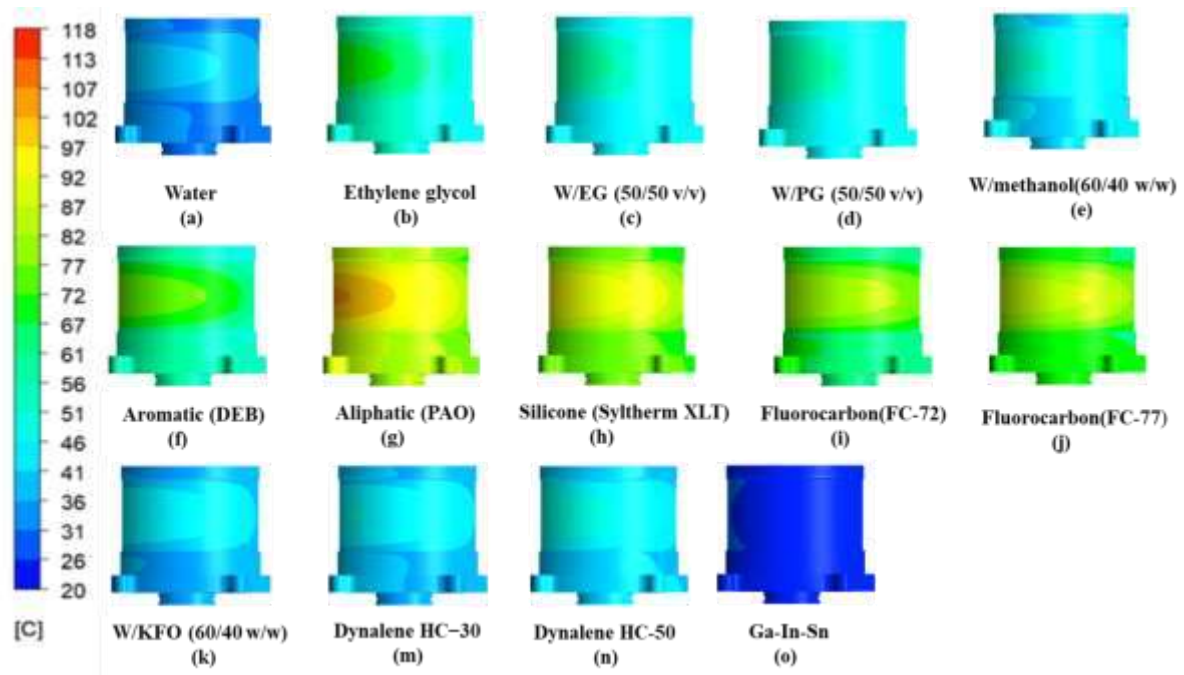


Figure 11. Temperature field of front bracket

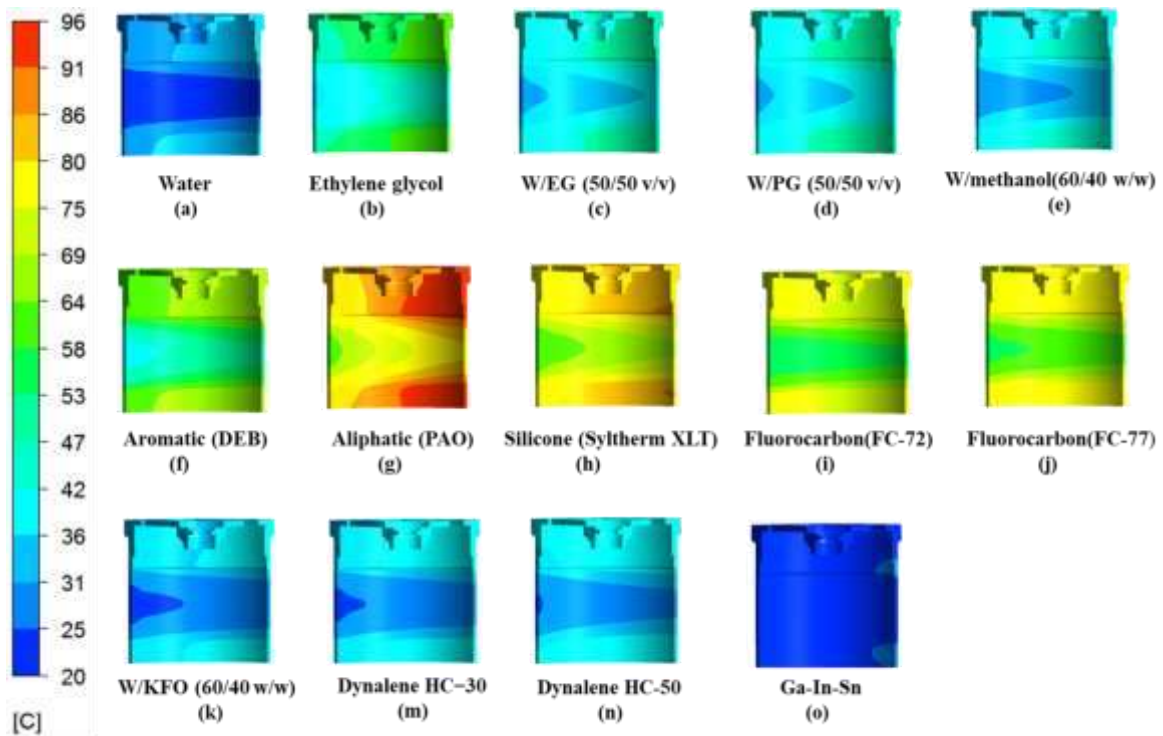


Figure 12. Temperature field of Rear bracket

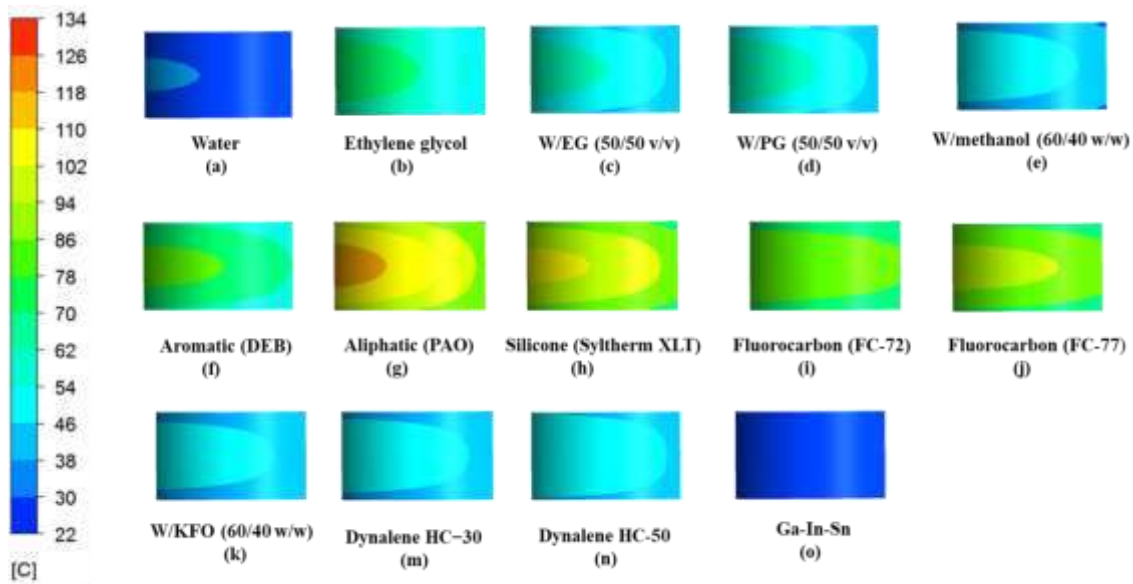


Figure 13. Temperature field of Stator Stack

8. Pressure drop of nanofluids

To apply the coolants for practical application, it is necessary to study their flow characteristics in addition to the heat transfer performance of the coolants. Adding nanoparticles to a base liquid can increase pressure loss due to increased viscosity and therefore increase the necessary pumping energy for moving of the nanofluids in the fluid passage. Ethylene glycol observed to have maximum pressure drop of 33 mbar when compared with other coolants which is higher than the limit of 25 mbar. Aromatic coolants observed to have minimum pressure drop of 1.6 mbar. For the remaining coolants, pressure drop falls in the range of 10-2.5 mbar. As shown in figure 14, the pressure drops of the coolants increase with increasing viscosity of fluid. This means that using the nanofluids at higher viscosity may create high-pressure drop.

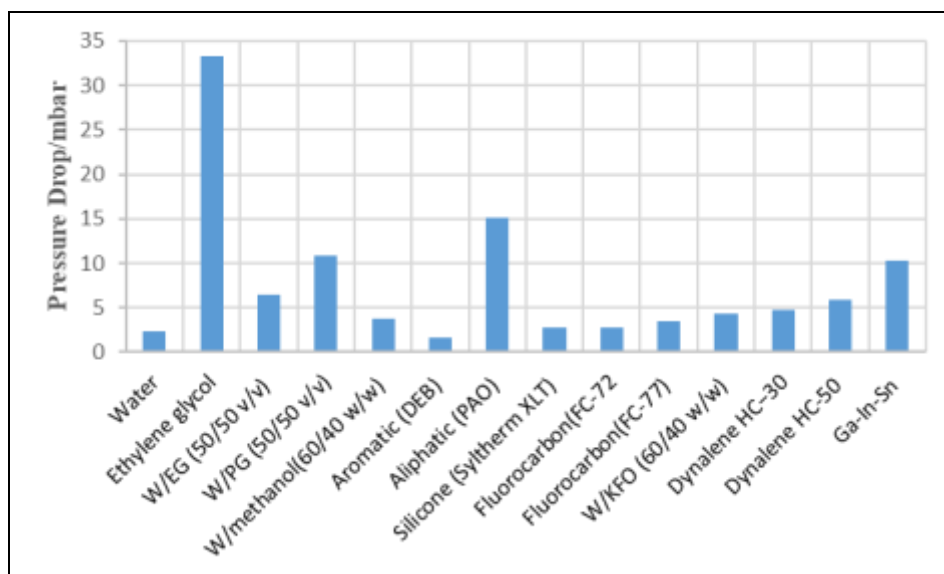


Figure 14. Influence of nanofluids on pressure drop

9. Conclusion

In conjugate heat transfer condition, a 3-D quarter electric motor model evaluated numerically to explore fluid flow and heat transfer efficiency through distinct kinds of operating fluids, i.e. water and multiple kinds of nanofluids. The effectiveness of E-machines measured with respect to temperature profile, pressure drop, and thermal resistance.

The highest temperature encountered at the front bracket wall where the constant heat source applied to the stator stack. Ga-In-Sn provided 30% temperature reduction compared to other nanofluids. Increased thermal conductivity reduced the temperature at the heated surface of brackets. The outcome of the research work show that the enhanced heat transfer obtained by Ga-In-Sn, which has a higher thermal conductivity. Indeed, the findings calculated showed that Ga-In-Sn's heat transfer effectiveness is better than pure water performance. In this condition, it suggested that Ga-In-Sn improve general heat transfer.

References

- [1] G. Karimi-Moghaddam, R. D. Gould, S. Bhattacharya, and D. Tremelling 2014 *Thermomagnetic liquid cooling. A novel electric machine thermal management solution.* (IEEE Energy Conversion Congress and Exposition ECCE) pp 1482–1489
- [2] T. Davin, J. Pellé, S. Harmand, and R. Yu 2015 *Experimental study of oil cooling systems for electric motors* (Applied Thermal Engineering) pp 75:113
- [3] H. Matsuzaki, Y. Kimura, I. Ohtani, M. Izumi, T. Ida, Y. Akita, et al. 2005 *An axial gap-type HTS bulk synchronous motor excited by pulsed-field magnetization with vortex-type armature copper windings*, (IEEE Trans. Appl. Supercond.) pp 2222–2225
- [4] T. Davin, J. Pelle, S. Harmand, R. Yu 2015 *Experimental study of oil cooling systems for electric motors* (Appl. Therm. Eng.) pp 75: 1–13
- [5] D. Lim, S. Kim 2014 *Thermal performance of oil spray cooling system for in-wheel motor in electric vehicles* (Appl. Therm. Eng.) pp 577–587
- [6] J. King, R. Kobuck, J. Repp 2005 *High-speed water-cooled permanent magnet motor for pulse alternator-based pulse power systems* (IEEE Trans. Appl. Supercond.) pp 2222–2225
- [7] M.S. Kim, K.W. Lee, S. Um 2009 *Numerical investigation and optimization of the thermal performance of a brushless DC motor* (Int. J. Heat Mass Transf.) pp 1589–1599
- [8] Z. Huang, F. Marquez, M. Alakula, J. Yuan 2012 *Characterization and application of forced cooling channels for traction motors in HEVs* (IEEE Conference on Electrical Machines) pp 1212–1218
- [9] I. Mudawar, D. Bharathan, K. Kelly, S. Narumanchi 2012 *Two phase spray cooling of hybrid vehicle electronics* (IEEE Trans. Compon. Packag. Technol.) pp 1480–1485
- [10] Z. Karim, A. Yusoff 2014 *Cooling system for electric motor of electric vehicle propulsion* (Adv. Mater. Res.) pp 209–214
- [11] F. Zhang, S. Song, G. Du, Y. Li 2013 *Int. Conf. on Electrical Machines and Systems Analysis of the 3D steady temperature field of MW high speed permanent magnet motor* (International Conference on Electrical Machines and Systems) pp 1351–1354
- [12] Mohapatra SC 2006 *An overview of liquid coolants for electronics cooling* (Electronics Cooling) pp 560-568
- [13] Mohapatra S, Loikits D. *Proc. Symp. Advances in liquid coolant technologies for electronics cooling* (IEEE semiconductor thermal measurement and management) pp 354–60
- [14] Simons RE. 1996 *Direct liquid immersion cooling for high power density microelectronics* (Electron Cool)
- [15] Murshed SMS, Leong KC, Yang C. 2008 *Investigations of thermal conductivity and viscosity of nanofluids* (International Journal thermal science) pp 560–8

- [16] Murshed SMS. 2012 *Simultaneous measurement of thermal conductivity, thermal diffusivity, and specific heat of nanofluids* (Heat Transfer Engineering) pp 722–31
- [17] Lee, J.L.S.J., 1999 *Stagnation region heat transfer of a turbulent axisymmetric jet impingement*. (Experimental Heat Transfer) pp 137-156
- [18] J. M. Kay, R. M. Needleman 1985 *Fluid Mechanics and Transfer Processes* p 221
- [19] R. Byron Bird, Warren E. Stewart, Edwin N. Lightfoot 2006 *Transport Phenomena* (John Wiley & Sons)